Catalysis Today xxx (2016) xxx–xxx

Contents lists available at ScienceDirect

Catalysis Today

journal homepage: www.elsevier.com/locate/cattod

Growth of TiO_2 nano-wall on activated carbon fibers for enhancing the photocatalytic oxidation of benzene in aqueous phase

Ajit Sharma, Byeong-Kyu Lee*

Department of Civil and Environmental Engineering, University of Ulsan, Nam-gu, Daehak ro 93, Ulsan 680-749, Republic of Korea

ARTICLE INFO

Article history:
Received 9 June 2016
Received in revised form 7 October 2016
Accepted 6 November 2016
Available online xxx

Kewords:
ACFs
TiO_2
Nano-wall
UV light
Photo-oxidation
Benzene

ABSTRACT

In the present study, TiO_2 nano-wall networks (TNWs) were successfully grown on the surface of activated carbon fibers (ACFs) pre-coated with TiO_2 nanoparticles (TNPs) via a hydrothermal process. The TNWs with an average length of 0.7–0.9 μm grew on the ACFs (ACF-TNW) surface in a three-dimensional direction to a complex structure with good uniformity and high crystallinity, as confirmed by scanning electron microscopy (SEM) and X-ray diffraction (XRD) analysis. The maximum removal capacities of benzene in a combined process of photo-oxidation and sorption affinity were 111.6 and 144.8 mg/g for ACF-TiO_2 and ACF-TNW, respectively, at pH 5, under UV light irradiation within 80 min. The highest benzene removal efficiency of 98.7% in the ACF-TNW system (in 100 mL of 50 mg/L), also confirmed by the CO_2 emission results, was accompanied by total organic carbon (TOC) and chemical oxygen demand (COD) reductions of 79.5 and 82.3%, respectively. The ACF-TNW nanocomposite also showed a higher photocatalytic oxidation of benzene than that of TNPs due to the minimization of electron-hole recombination resulting from the transfer of photo-induced electrons through the ACFs surface. The ACF-TNW nanocomposite was also easily separated from aqueous solution for regeneration and showed good stability after multiple uses.

1. Introduction

Benzene is a natural constitute of crude oil and an important component of gasoline because of its high octane number. The major sources of benzene in water are atmospheric deposition, spills of petrol and other petroleum products, and chemical plant effluents [1]. Levels of up to 179 μg/L have been reported in chemical plant effluents [2]. In seawater, levels were reported to be in the range 5–20 ng/L (coastal area) [3]. The U.S. National Primary Drinking Water Regulations has set a maximum contaminant level for benzene in drinking water at 0.005 mg/L (5 ppb) [4]. The maximum contaminant level goal, a non-enforceable health goal that would allow an adequate margin of safety for the prevention of adverse effects, is zero benzene concentration in drinking water. Unfortunately, many conventional treatment processes, such as membrane separation, and physiochemical methods, such as catalytic oxidation-reduction process and biological methods, are unable to minimize or neutralize the environmental harm of aquatic benzene [1,5–7]. Recently, benzene removal by a combination of sorption and catalytic oxidation-reduction processes has become a very attractive and promising alternative because of its high retention capacity, easy handling, and high benzene removal efficiency [8,9]. The separation of benzene molecules over water is often treated by a sorption method using carbon-based composites [10,11]. However, the relatively high initial and regeneration costs of such carbon-based composites have encouraged researchers to study the applicability of other more economic and environmentally friendly removal techniques.

Titanium dioxide (TiO_2) exhibits high photocatalytic activity under UV light irradiation with a bandgap of 3.2 eV, but its low quantum efficiency creates negligible utilization under visible phase [12,13]. The photocatalytic degradation of aqueous phase volatile organic compounds by titanium dioxide (TiO_2) is a relatively slow process with many limitations for industrial or large-scale applications. These limitations include safety issues, use of powder materials and high-energy consumption due to UV irradiation requirement [14–16]. Catalytic or sorbent-based powder materials cause channeling and flow problems in real industrial applications. Powder photocatalysts cannot be recycled easily and may cause secondary pollution [17]. Thus, it is desirable to prepare TiO_2 photocatalysts deposited on the support materials with high surface areas. Activated carbon fibers (ACFs) are a newly developed type of support material with a large surface area and its preparation has attracted research attention [18,19]. Shi et al. [20] reported

* Corresponding author.
E-mail addresses: bklee@ulsan.ac.kr, bklee.ulsan.kr@gmail.com (B.-K. Lee).

http://dx.doi.org/10.1016/j.cattod.2016.11.019
0920-5861/

that ACFs-supported TiO_2 exhibited high photocatalytic activity. Ao et al. [21] reported that Ag nanoparticles loaded TiO_2 array can be fabricated on ACFs and that the resulting composite exhibited excellent photocatalytic activity. However, no study has focused on the preparation and photocatalytic activity of metallic nanoparticle (NP)-coated ACFs on which TiO_2 nano-wall networks (TNWs) are grown.

The first aim of the present study is to prepare TiO_2-doped ACFs as a photocatalytic filter for the removal of benzene from aqueous environments. ACFs have been recognized for its multifunctional properties based on its hierarchical porous structure, high thermal and tensile stability [18]. ACFs are attractive due to its versatile roles as an adsorbent and catalyst, as well as a support material for metallic catalysts in environmental pollution remediation [22–24]. In the current study, the ACFs surface was modified by TiO_2 doping to improve the sorption affinity and photocatalytic property in the sorption-oxidation of aqueous benzene. To date, most of the TiO_2 nanostructures prepared on ACFs have been limited to amorphous TiO_2 NPs (TNPs) obtained by sol-gel process [25]. These amorphous TNPs are not crystalline, but a good crystalline structure needs to be formed for secure treatment at high temperature. Moreover, the quality of the resulting composite material is not good enough for photocatalysis/sorption because of its uneven surface, salt formation and blockage of porous structure [20,24,25].

Thus, the growth of TNWs on the ACFs surface can enhance the photocatalytic activity under UV light irradiation. Moreover, we hypothesized that the growth would increase the sorption affinity of the photocatalyst, thereby significantly enhancing the benzene removal rate by the combination of sorption and photodegradation. In addition, the ACFs surface modified with TNWs (ACF-TNW) may increase the photocatalytic activity by improving the electron transfer efficiency. In this study, TNWs were grown on the ACF surface and the phase structure, vibrational mode, doped metal oxide crystallinity, optical behavior and surface morphology of the resulting nanocomposite were investigated. The sorption affinity and photocatalysis of ACF-TNW were also analyzed by evaluating the sorption-oxidation of benzene under UV light irradiation.

2. Materials and methods

2.1. Chemicals used

Titanium (IV) isopropoxide (TIP) as a source of TNWs and benzene as a pollutant were purchased from Daejung Chemical and Metals Co. Ltd. All regents were prepared with double distilled H_2O using analytical grade chemicals. ACFs substrate was purchased from Osaka Gas Chemical Co., Ltd. (Japan). Before being used as the substrate for TNWs growth, the ACFs substrate was pretreated as follows. Firstly, the ACFs substrate was cut into small square pieces uniformly sized 2 cm × 2 cm, and then soaked in hydrochloric acid (1%) for 1.5 h to remove all impurities [18]. After washing several times with distilled water, the ACFs pieces were dried in a hot-air oven at 60 °C. The ACFs pieces were then placed in a nitrogen furnace at 120 °C for 2 h, and used in subsequent experiments.

2.2. Preparation of TiO_2 nanoparticle-deposited ACF

Titanium (IV) isopropoxide (TIP) (30 mL) was dissolved in 100 mL of ethanol with stirring for 20 min to obtain a homogeneous solution. The ACFs pieces sized 2 cm × 2 cm were used as the substrate for the deposition of TNPs. Then, the ACFs substrate was dipped in the homogeneous solution. After sonicating for 20 min, the ACFs substrate was taken out and washed with ethanol to remove any excess TIP precursor between the fibers and then dried at 80 °C for 12 h. In order to enhance the TiO_2 crystallization, TiO_2-doped ACFs was calcined at 600 °C in nitrogen atmosphere for 2 h to afford the ACF-TiO_2 sample.

The TNPs were synthesized using the above procedure except that no ACFs pieces were added [12].

2.3. Growth of TiO_2 nano-wall networks (TNWs) on ACF

Sample pieces of ACF-TiO_2 were put into 80 mL of 10 M NaOH aqueous solution, then transferred into a 100 mL Teflon-lined stainless steel autoclave, and sealed. The autoclave was put into an oven, heated at 140 °C for 20 h, cooled naturally in air and washed with deionized water several times until the sample pH reached 7. The morphological structure of TNWs on the ACFs surface (ACF-TNW) was determined by surface morphology analysis.

2.4. Instruments

The surface morphology for monitoring of the TNWs growth was analyzed by Hitachi S-4700 scanning electron microscopy (SEM). Semi-quantitative analyses for elemental composition of the ACFs surface were performed on an energy-dispersive X-ray (EDX) spectrometer connected to a Hitachi S-4700. Differences in the light absorption spectra of TiO_2, ACF-TiO_2 and ACF-TNW were identified by comparing UV–vis absorption spectra at 300–800 nm wavelengths using a UV–vis spectrophotometer (UV-1700 Shimadzu). The crystallinity of the TiO_2 and ACF-TNW surfaces was characterized by X-ray diffraction (XRD, Bruker AXN) in the 2θ range of 5–80°. The chemical oxidation states of ACF-TNW were characterized by X-ray photoelectron spectroscopy (XPS, Thermo Scientific K-Alpha XPS spectrometer).

Stock solutions of benzene were prepared in the concentration range of 2 to 50 mg/L with double distilled H_2O. The concentrations of benzene were determined by UV–vis spectrophotometry (Genesys 10S UV–vis spectrophotometer, Thermo Scientific) at the wavelength (λ_{max}) range of 190–212 nm [1].

Analysis of chemical oxygen demand (COD) was used to express the COD of benzene solution before and after the photo-oxidation. The total organic carbon (TOC) of the benzene solution was determined by TOC 500 A (Shimazu, Japan). The mineralization efficiency of complete benzene removal was measured by a carbon dioxide (CO_2) analyzer (Alpha Omega Instruments 9510 analyzer).

2.5. Oxidation-sorption of benzene

The complete removal of benzene using TiO_2, ACF, ACF-TiO_2 and ACF-TNW as photocatalytic sorbent materials was carried out under optimized pH conditions in a temperature-controlled water bath shaken at 110 rpm and 30 °C for 2 h under UV light irradiation and dark phase. Photocatalysis was executed in a thermostatic water bath equipped with UV lamps (Superstar Dulux EL, 20 W). The distance between the light source and the photocatalyst was 20 cm. The power density in the reaction chamber was 0.05 W/cm^2. For the pH optimization test, the pH levels were adjusted in the range of 2 to 10 using 0.1 N HCl or NaOH. The ACF-TNW pieces sized 2 cm × 2 cm were added into 100 mL of the benzene solution. The reaction solution was exposed in the presence of UV light at room temperature before starting the reaction. After the reaction, the flask was shaken for the desired time in UV light irradiation and dark phase. The reaction solution was filtered through a Whatman 0.45 μm filter membrane. The aqueous benzene concentration was evaluated by measuring the intensity of absorption peak at 190–212 nm using a UV–vis spectrophotometer [1]. The time equilibration was determined using 100 mL of benzene solution at concentrations of 20 and 50 mg/L, containing 2 cm × 2 cm sized ACF-TNW pieces under UV light irradiation, and the reaction times with shaking varied

Please cite this article in press as: A. Sharma, B.-K. Lee, Growth of TiO_2 nano-wall on activated carbon fibers for enhancing the photocatalytic oxidation of benzene in aqueous phase, Catal. Today (2016), http://dx.doi.org/10.1016/j.cattod.2016.11.019

from 0.1 to 3 h. The effects of various experimental design parameters, such as the effect of H_2O_2, on the benzene oxidation were also examined under UV light irradiation. The used ACF-TNW composite was treated with H_2O_2, washed by deionized water with ethanol and dried at 80 °C for regeneration experiment under identical conditions. The molecules of benzene removed per gram of TiO_2, ACF, ACF-TiO_2 and ACF-TNW were calculated by the difference between the initial and the final benzene concentration using Eq. (1) [12].

$$q_e = (C_o - C_e) \times V/W \quad (1)$$

The benzene removal efficiency after the photo-oxidation and the mineralization efficiency of benzene were calculated using the following Eqs. (2) and (3), respectively [1,9]:

$$\text{Removalefficiency}(\%) = [C_o - C_e/C_o] \times 100 \quad (2)$$

$$\text{Mineralization}(\%) = [CO_2\text{produced}/\text{benzeneconversion}] \times 100 \quad (3)$$

where q_e is the amount of the eliminated benzene molecules (mg/g) on TiO_2, ACF, ACF-TiO_2 and ACF-TNW, C_o the initial concentration of benzene (mg/L), C_e the equilibrium concentration of benzene (mg/L), V the volume of the benzene sample solution used (L), and W (g) the weight of TiO_2, ACF, ACF-TiO_2 and ACF-TNW used. A blank solution (no addition of sorbent-catalyst) was used in all experiments to evaluate the amount of evaporation loss of benzene during the study. A cap-closed reaction flask was used to control the evaporation loss of benzene during the oxidation-sorption process.

3. Results and discussion

3.1. Materials characteristics

3.1.1. Morphology and elemental compositions

The morphology and elemental compositions of ACF, ACF-TiO_2 and ACF-TNW were analyzed by SEM/EDX analysis (Fig. 1). As shown in Fig. 1(a), the ACFs surface was almost clean after pretreatment with many micropores that can function as active sites for adsorption. Fig. 1(b) shows SEM images of the ACF-TiO_2 compos-

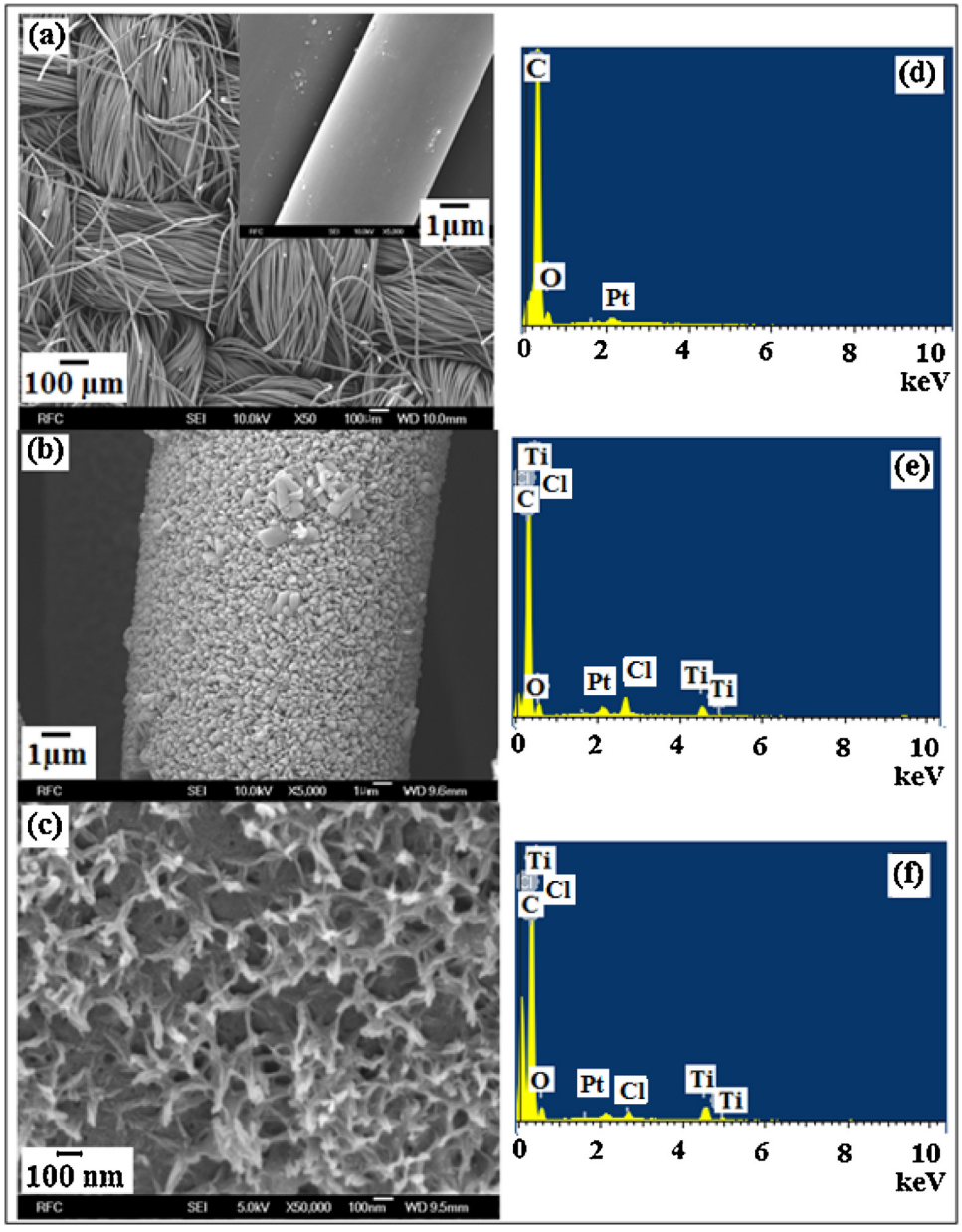

Fig. 1. SEM and EDX analysis of ACF (a, d), ACF-TiO_2 (b, e) and ACF-TNW (c, f), respectively.

Please cite this article in press as: A. Sharma, B.-K. Lee, Growth of TiO_2 nano-wall on activated carbon fibers for enhancing the photocatalytic oxidation of benzene in aqueous phase, Catal. Today (2016), http://dx.doi.org/10.1016/j.cattod.2016.11.019

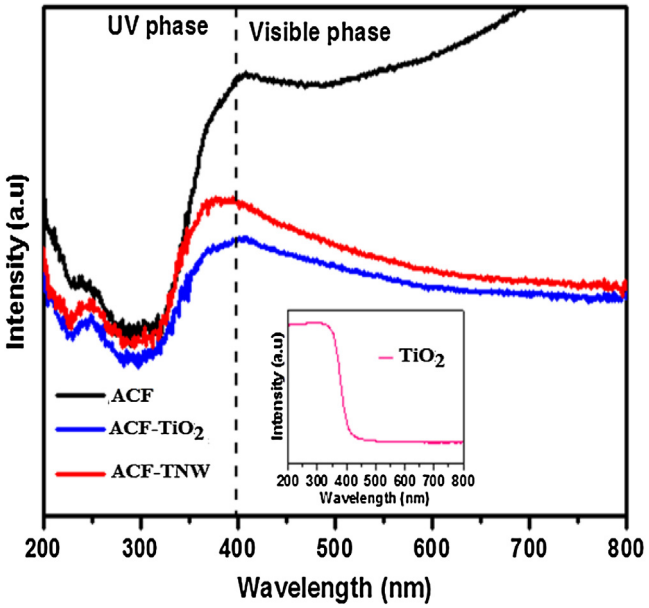

Fig. 2. UV–vis spectra of all samples.

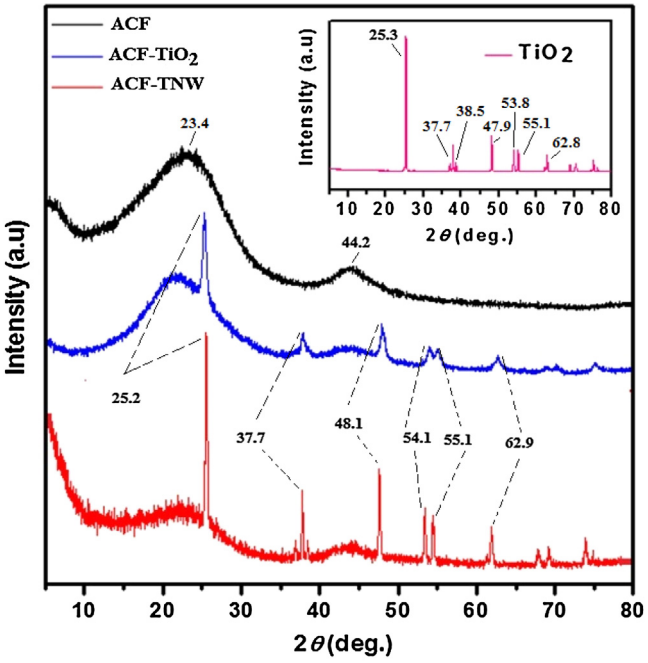

Fig. 3. XRD patterns of all samples tested.

ite prepared by the sol gel process. TNPs were uniformly deposited on the ACFs surface. As shown in Fig. 1(c), the growth of TNWs on the ACFs surface is in three-dimensional direction to a complex structure was produced. The TNW structures with an average length of 70–90 nm were confirmed in the SEM image (Fig. 1c). The highly uniform TNWs structures of TiO_2 were deposited on the ACFs surface with high crystallinity. The TNWs structures of TiO_2 on the ACFs surface exhibited great adsorption capacity and photocatalytic activity for complete oxidation of benzene from aqueous media. In the EDX spectra of ACF, ACF-TiO_2 and ACF-TNW (Fig. 1d–f, respectively), the elemental peaks of Ti, O, and C were attributed to the TiO_2 doping on the carbon-based ACF surface. In addition, Ti peaks were not observed on the surface of the parent ACF. However, other elements such as Pt and Cl originated from SEM-EDX sample characterization processes.

According to the SEM morphology of ACF-TNW (Fig. 1c), the growth of TiO_2 nano-wall network on to ACF was obtained by the "dissolve and grow" method [27]. In the reaction process, the NaOH played as a reactant to dissolve Ti and also act to control the hydrolysis rate of Ti(III) by providing an alkaline environment. In the presence of NaOH, Ti reacts with H^+ at high temperature and pressure and gradually dissolves, continually releasing the Ti(III) precursors into the reaction solution. Thus, $TiOH^{2+}$ is produced by hydrolysis of Ti(III) because Ti(III) is unstable in aqueous solution and $TiOH^{2+}$ is oxidized to Ti(IV) by reaction with dissolved oxygen. The Ti(IV) complex ions are thus used as the growth units with chainlike cluster structures, and thus, a large number of the polycrystalline cluster structures are formed in the solution by homogeneous nucleation. Subsequently, these cluster structures are deposited on the ACF surface and act as the nucleating centers for further growth of TiO_2 nano-wall network. This may be attributed to the good bonding force and low surface tension between the ACF surface and TiO_2 nano-wall network.

3.1.2. Optical absorption

Fig. 2 shows the optical absorption in the range of 200–800 nm of the synthesized TNPs, ACF, ACF-TiO_2 and ACF-TNW materials. As shown in Fig. 2, the spectra of TiO_2 indicated absorption in the UV region at 360–405 nm, which can be attributed to photo-excitation from a valence band to a conduction band of TiO_2 [28]. However, UV–vis absorption spectra of ACF show that carbon-based ACF can completely absorb UV and visible irradiation [20]. Therefore, ACF, ACF-TiO_2 and ACF-TNW exhibited strong absorption throughout the UV–Vis wavelength range employed due to the carbon-based black color of ACFs. In the spectra of the ACF-TiO_2 and ACF-TNW materials, absorbance in the UV region was higher than in the visible region due to the TiO_2 metal oxide deposition on the ACFs surface. However, the absorption of ACF-TNW was greater than that of ACF-TiO_2. The slight increase in the absorbance of ACF-TNW following TNWs growth may have been due to obstruction of the light by the nano-wall structures [21]. In addition, ACF-TNW had increased absorption at 400–500 nm, indicating enhancement of the photocatalytic properties in the UV phase compared to TiO_2. The light absorption was increased by the interaction of the carbon basal surface of ACFs with TiO_2. This indicates that ACFs, having a conjugated structure, enhanced the charge separation in the electron-transfer processes [18,26]. Furthermore, this can be attributed to charge transition transfer and excited photon energy reduction, which combined to give UV–vis lower absorption than that of TiO_2. These UV–vis spectra results suggest that ACF-TNW has photocatalytic activity under UV light irradiation. Thus, the photocatalytic activity of TiO_2 and adsorption by ACFs facilitate complete removal of benzene from aqueous media.

3.1.3. Crystallography

XRD was used to analyze the crystallinity and phase composition of the TNP, ACF, ACF-TiO_2 and ACF-TNW materials (Fig. 3). Major XRD peaks of the synthesized TNPs were observed at 2θ of 53.8°, representing the rutile phase, while the peaks at 2θ values of 25.3°, 37.7°, 38.5, 47.9°, 55.1°, 62.8° 68.6° 70.3° and 75.1° indicated the anatase phase of TNPs [12,28]. In the XRD patterns of ACF, however, the major peaks at 2θ of 23.4° and 44.2° are attributed to the crystalline plane of amorphous carbon [18]. Furthermore, all the XRD patterns of the ACF-TiO_2 and ACF-TNW composite materials showed the typical peaks of a TiO_2 crystalline structure and crystalline plane of amorphous carbon, indicating the presence of TiO_2 doping in the carbon texture of ACFs. This crystalline characteristic indicates that the texture of ACFs was not damaged by TiO_2 fabrication. However, all peaks in the XRD patterns of ACF-TNW have higher intensity with better crystalline structure than those

Please cite this article in press as: A. Sharma, B.-K. Lee, Growth of TiO_2 nano-wall on activated carbon fibers for enhancing the photocatalytic oxidation of benzene in aqueous phase, Catal. Today (2016), http://dx.doi.org/10.1016/j.cattod.2016.11.019

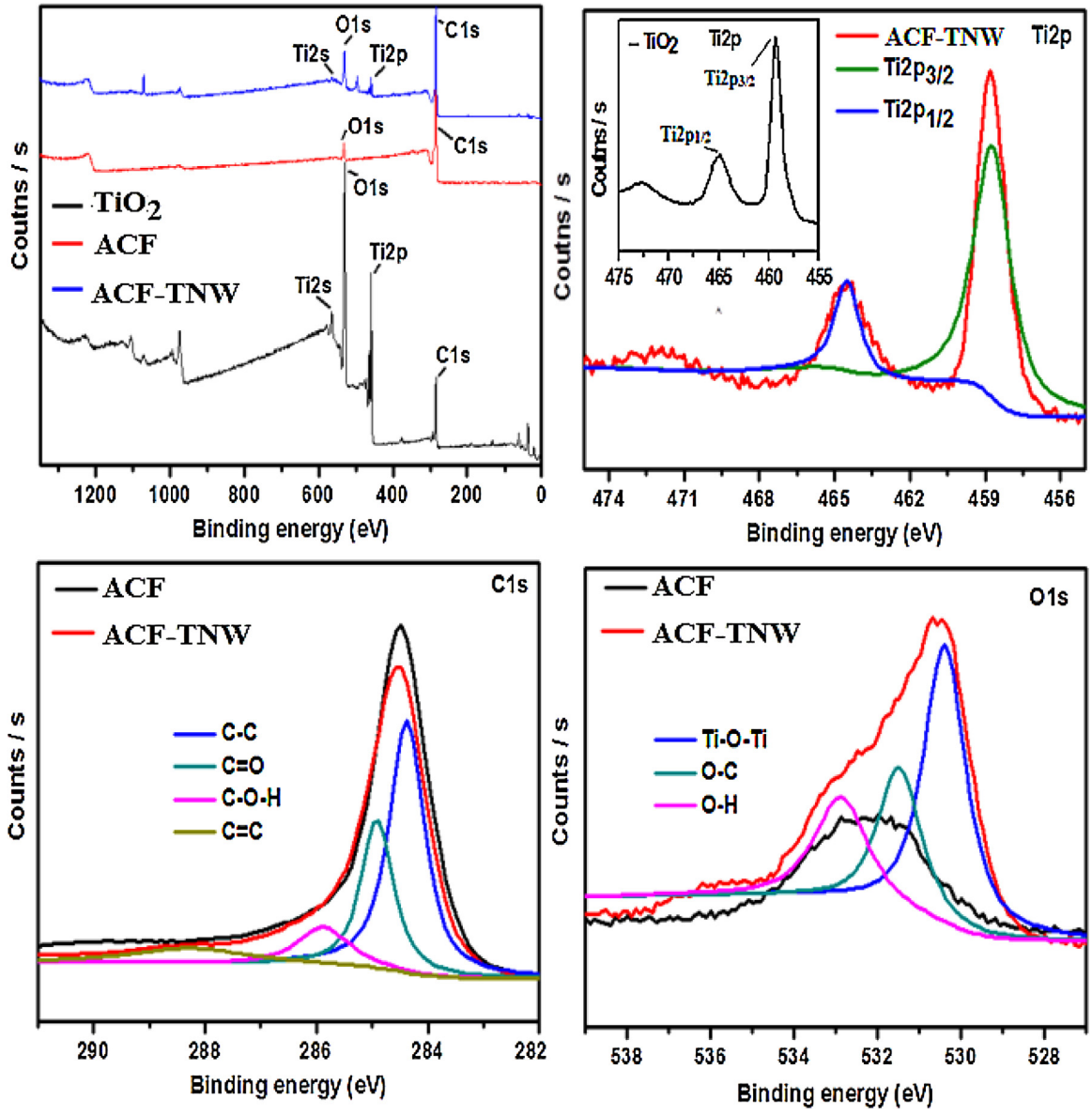

Fig. 4. XPS core-level spectra of all samples tested.

of ACF-TiO_2. Therefore, ACF-TNW provides better photocatalytic properties that can generate more electron-hole pairs for the oxidation of benzene during irradiation with UV light and the porous carbon surface in ACF-TNW provides more sorption ability.

3.1.4. Chemical oxidation states

The chemical oxidation states of TNPs, ACF and ACF-TNW were elucidated based on the core level XPS spectra. The full range of XPS spectra (0–1300 eV) of TiO_2, ACF and ACF-TNW are shown in Fig. 4. The TiO_2 and ACF-TNW hierarchical hetero-structures are composed of C, O and Ti. No significant impurities were observed in the XPS spectra of ACF-TNW. However, the oxygen peak in the XPS spectra of ACF was less intense than that of TiO_2 and no Ti elements were observed. In the Ti2p core, the binding energies (BE) at 464.9 eV and 459.3 eV were accredited to the $2p_{1/2}$ and $2p_{3/2}$ peaks of TiO_2, respectively, indicating that the ionic state of TiO_2 was Ti^{+4} [12,28]. The XPS spectra of TiO_2 also presented the narrow and sharp shape of the Ti 2p peaks, indicating that all the titanium in TNPs existed in the Ti^{+4} state [9]. The binding energy of the $Ti2p_{1/2}$ peaks in ACF-TNW slightly diverged from 464.9 eV (in TiO_2) to 464.5 eV. In addition, the Ti2p peaks of TiO_2 in ACF-TNW were less intense than those in TNPs, implying that the ionic state of TiO_2 was not simply Ti^{4+} in both composites. Subsequently, the multi-peak shapes of the Ti 2p peaks of titanium in ACF-TNW revealed that they were composed of a combination of Ti^{3+} and Ti^{4+} peaks. The formation of Ti^{3+} in ACF-TNW was due to the reduction of Ti^{4+}, which could be attributed to the crystalline plane of amorphous carbon of the ACF surface [20,32]. In the C1s core level, the leading peaks were observed at 284.4 and 284.5 eV for ACF and ACF-TNW, respectively. The peak for ACF-TNW showed less intensity than that of ACF. Additionally, the XPS spectrum of C 1s core level was resolved into four individual peaks representing carbon associations: C—C (BE = 284.3 eV), C=O (BE = 284.8 eV), C—O—H (BE = 285.8 eV) and C=C (BE = 288.3 eV) [33]. In the O1s core level, the leading peaks were observed at 530.6 and 532.1 eV for ACF-TNW and ACF, respectively. The peak intensity for ACF-TNW was broader and stronger compared to that for ACF. In addition, the asymmetric spectrum of oxygen in ACF-TNW evidently indicated the presence of multicomponent oxygen species on the surface. Three chemical states of oxygen corresponding to Ti—O—Ti

Please cite this article in press as: A. Sharma, B.-K. Lee, Growth of TiO_2 nano-wall on activated carbon fibers for enhancing the photocatalytic oxidation of benzene in aqueous phase, Catal. Today (2016), http://dx.doi.org/10.1016/j.cattod.2016.11.019

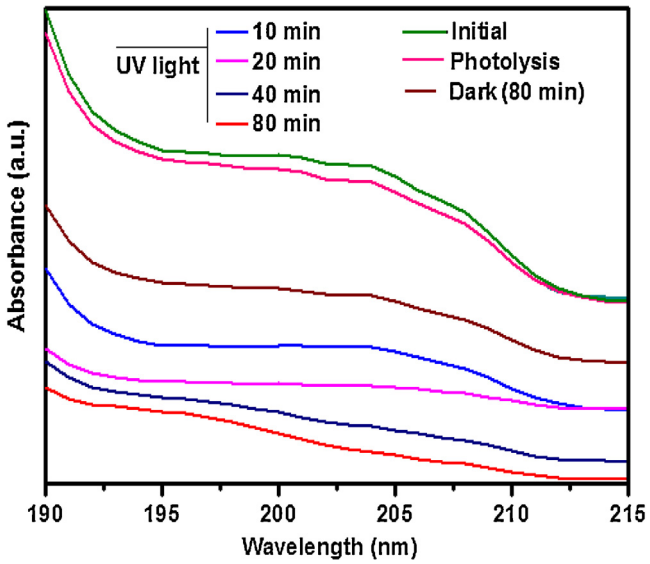

Fig. 5. UV–vis absorption spectra of benzene solutions according to duration of contact with ACF-TNW.Concentration of benzene = 50 mg/L, amount of ACF-TNW = 2 cm x 2 cm, reaction volume = 100 mL, reaction time = 80 min, temperature = 30 °C..

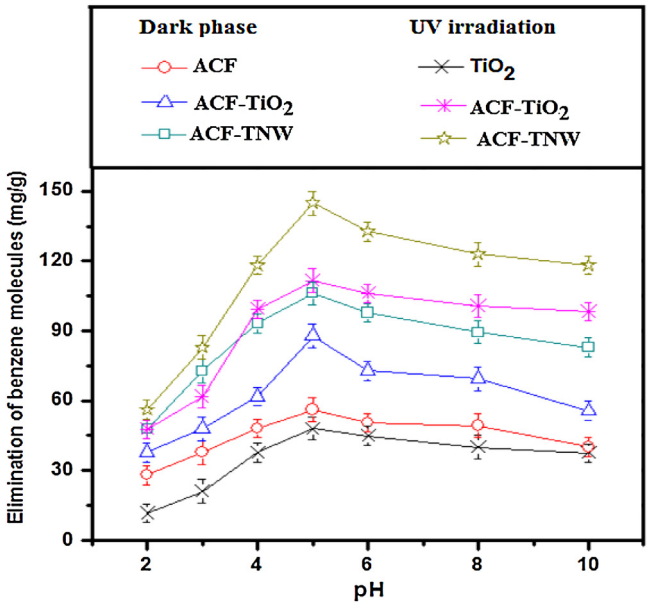

Fig. 6. Effect of solution pH on the photo-oxidation and sorption of benzene under dark phase and UV light irradiation.
Concentration of benzene = 50 mg/L, amount of samples = 0.01 g of TiO_2 powder and size of ACF, ACF-TiO_2 and ACF-TNW = 2 cm × 2 cm (equal to 0.01 g of TiO_2 powder), reaction volume = 100 mL, H_2O_2 = 0.1%, reaction time = 80 min, temperature = 30 °C.

(BE) = 530.3 eV), O—C (BE = 531.5 eV) and O—H (BE = 532.8 eV) were detected [34]. The hydroxyl groups of water molecules absorbed on the composite surface could function as electron donors for photo-generation of H^+ and be oxidized into hydroxyl radicals (•OH), which play the key role in the photo-oxidation of benzene molecules [9,20,32].

3.2. Oxidation-sorption of benzene

3.2.1. Temporal photo-oxidation

In order to explore the reaction mechanism, a kinetic study was carried out for ACF-TNW. Fig. 5 shows the UV–vis absorbance values of benzene during photocatalytic oxidation. Without adding any photocatalyst samples, the benzene degradation was negligible even under UV light irradiation. This indicates that photolysis is not effective for benzene degradation [1]. The reaction mixture was stirred under dark condition for 80 min to attain adsorption–desorption equilibrium between benzene and ACF-TNW. When the reaction solution was irritated under UV light for different times (10, 20, 40, 80 min), the benzene peak significantly decreased or almost disappeared with increasing UV light irradiation. This observation indicates that the time must be optimized to generate the electrons and holes (e^-/h^+) that are required to initiate the complete photo-oxidation of benzene.

3.2.2. pH effect

Fig. 6 depicts the influence of pH on the oxidation-sorption removal of benzene by TNPs, ACF, ACF-TiO_2 and ACF-TNW under UV light irradiation and dark phase. For all the sorbent samples, the benzene elimination efficiency was very low in strongly acidic media ($pH \leq 2$) and relatively low in basic media ($pH > 7$) as compared to that in weakly acidic conditions around pH 5. The benzene elimination was maximized at pH 5, with maximum removal capacities of 56.6, 87.8, and 106.2 mg/g for ACF, ACF-TiO_2 and ACF-TNW, respectively, under dark condition. Under UV light irradiation, the maximum amount of removed benzene was 9.6, 111.6, and 144.8 mg/g for TiO_2, ACF-TiO_2 and ACF-TNW, respectively, at pH 5. These values were greatly improved as compared those in dark phase. The surface charge of the sorbent-catalyst is mainly responsible for benzene removal [35]. The zero point of charge (pHzpc) of benzene was 4.45, which is lower than that of ACF-TNW (pHzpc = 8.2). In the strongly acidic solutions ($pH \leq 4$), the whole surface of the sorbent-catalyst becomes mostly positive charged and thus produces an electrostatic repulsion towards the acidic moiety of benzene [36]. The ACF-TNW has a greater anionic charge at pH 5 or higher pH. Thus, the improved sorption of benzene at pH 5 is because the acidic form of benzene and ACF-TNW with anionic charge has a strong electrostatic attraction that improves the sorption ability. However, at pH 6, benzene has a relatively lower acidic form and relatively less electrostatic attraction than those at pH 5, resulting in relatively decreased sorption ability. At alkaline pH, the whole surface of the sorbent-catalyst becomes negatively charged and an electrostatic repulsion toward the negatively charged benzene dominates [35]. Additionally, at alkaline pH, the removal capacity is decreased due to the competitive sorption onto the sorbent between adsorbate molecules and hydroxide ions. In the presence of UV light irradiation, the ACF-TNW surface was hydrated with –Ti—O—Ti and Ti—O—C [28]. It is also possible that OH^-/H_2O reacted with localized holes through electron transfer process to generate numerous hydroxyl radicals that can enhance the benzene oxidation under UV light irradiation [37].

3.2.3. H_2O_2 effect

Fig. 7 shows the photocatalytic activity of ACF-TNW in the photo-oxidation of benzene under UV light irradiation in the presence and absence of H_2O_2. H_2O_2 can provide more •OH radicals, thereby enhancing the photo-oxidation with formation of colored intermediates during photocatalysis. The test run of benzene photo-oxidation was conducted over a range of added H_2O_2 (30%) from 0.01 and 0.2% in 100 mL of benzene solution (50 mg/L), under UV light irradiation. The photo-oxidation efficiency was 47.9% without H_2O_2 addition. As the concentration of H_2O_2 was increased from 0.01 to 0.1%, the photo-oxidation of benzene increased from 86.5 to 95.3%. Further increase in the H_2O_2 concentration up to 0.2% resulted in a decrease to 72.1% degradation. H_2O_2 can trap photo-induced e^- to stabilize the paired e^-/h^+, which is attributed to the combination of photo-Fenton and photocatalytic reactions occurring on the ACF-TNW surface to generate more active radicals in aqueous medium. The •OH radicals could be generated via reac-

Please cite this article in press as: A. Sharma, B.-K. Lee, Growth of TiO_2 nano-wall on activated carbon fibers for enhancing the photocatalytic oxidation of benzene in aqueous phase, Catal. Today (2016), http://dx.doi.org/10.1016/j.cattod.2016.11.019

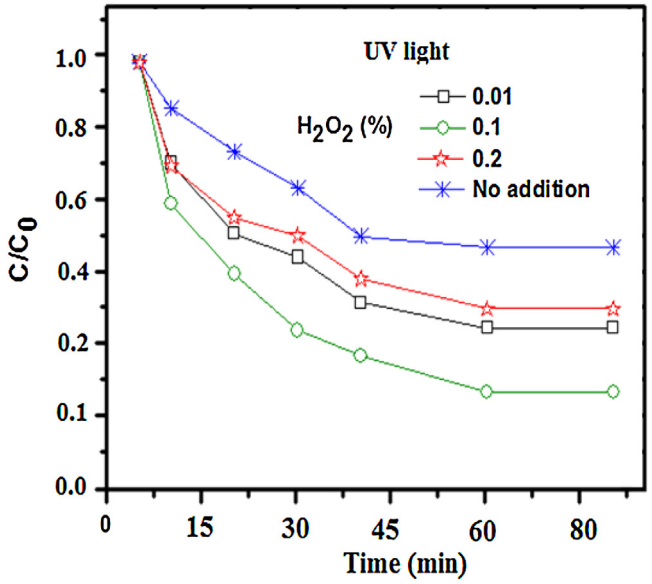

Fig. 7. Effect of H_2O_2 addition to ACF-TNW on the photo-oxidation of benzene under UV light irradiation.
Concentration of benzene = 50 mg/L, amount of ACF-TNW = 2 cm × 2 cm, reaction volume = 100 mL, reaction time = 80 min, temperature = 30 °C.

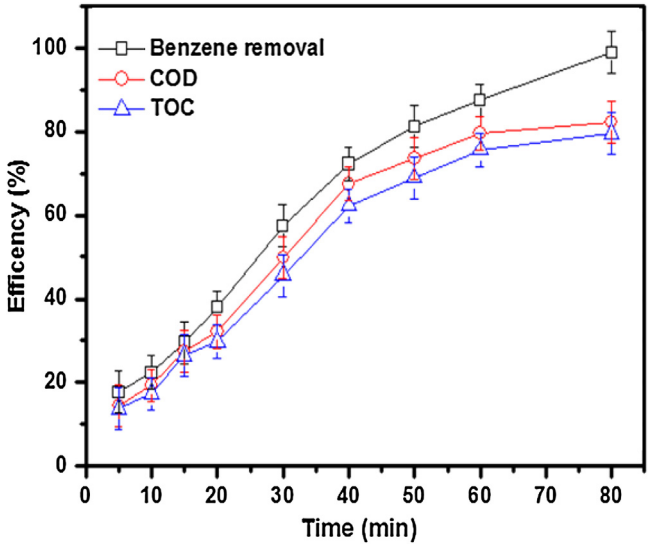

Fig. 8. Variations in TOC, COD and benzene removal efficiency according to duration of UV light irradiation.
Concentration of benzene = 50 mg/L, amount of ACF-TNW = 2 cm × 2 cm, reaction volume = 100 mL, H_2O_2 = 0.1%, reaction time = 80 min, temperature = 30 °C.

tion between H_2O_2 and e^- or $O_2^{\bullet -}$ [1,38]. Therefore, the addition of H_2O_2 to ACF-TNW enhanced the benzene oxidation by minimizing the recombination of electrons and holes with the generation of more •OH radicals. As the H_2O_2 concentration further increased, the additional H_2O_2 trapped the •OH radicals generated to form weaker oxidant $HO_2^{\bullet}$ radicals. Thus, the addition of excess H_2O_2 decreases the amount of •OH radicals and acts as an inhibitor [28].

3.2.4. Degree of mineralization

Fig. 8 shows the degree of benzene mineralization by photo-oxidation using ACF-TNW as a function of irradiation of UV light with variations of TOC and COD. After only 80 min irradiation under UV light, benzene photo-oxidation efficiency by ACF-TNW of 98.8% was achieved with a maximum reduction in COD and TOC of 82.3 and 79.5%, respectively. The benzene mineralization was also confirmed by CO_2 emissions during the photo-oxidation of benzene (Fig. 9). The emission concentration of CO_2 gradually increased with increasing irradiation time up to 50 min, but decreased slowly after that. This decrease in CO_2 concentration emitted indicates a decrease in the benzene mineralization rate after 50 min because of the decrease in benzene molecules available for the photo-oxidation, resulting in low conversion of benzene to CO_2 [1,39].

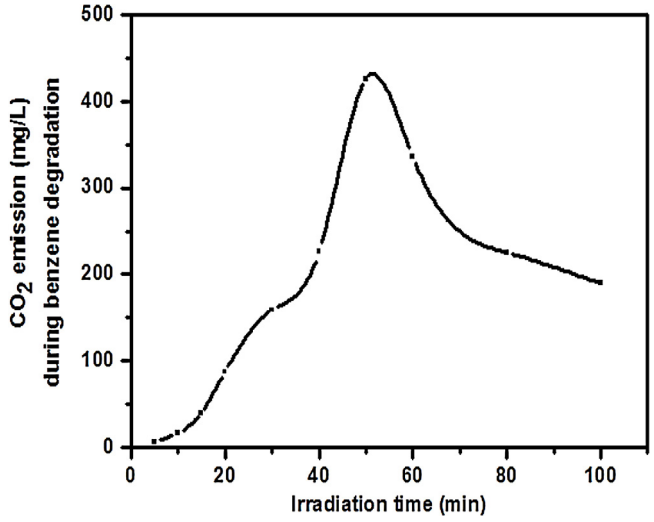

Fig. 9. Evolution of CO_2 emission with variable UV light irradiation time.
Concentration of benzene = 50 mg/L, amount of ACF-TNW = 2 cm × 2 cm, reaction volume = 100 mL, H_2O_2 = 0.1%, reaction time = 80 min, temperature = 30 °C.

3.2.5. Reusability and stability

The ACF-TNW nanocomposite was reused in 'n' number of cycles to evaluate its physical stability and economical use for the photo-oxidation of benzene. ACF-TiO_2 has more active sites where the photo-generated charge carriers react with absorbed molecules to form hydroxyl and superoxide radicals. However, powder-based TiO_2 material reduces the number of active sites during regeneration experiment handling, which decreases the photocatalytic efficiency. These drawbacks can be overcome by forming nano-wall structures on the ACFs surface via a facile process. After being used for benzene photo-oxidation, ACF-TNW in fiber form can easily be separated from the reaction solution and re-activated for further process. The re-activation or regeneration test was conducted by treating ACF-TNW (2 cm × 2 cm/10 mL) with 30% H_2O_2 solution for 30 min. The removal efficiency of benzene was 36% in the 4th cycle and removal efficiency of benzene was decreased with increasing number of regeneration cycles up to the fourth cycle (Fig. 10). The H_2O_2 treatment can remove the surface-trapped compounds by oxidizing them to H_2O and CO_2, thereby providing free active sites and a negatively charged surface [24,28]. This result indicated that ACF-TNW was stable and exhibited a high photocatalytic performance over four utilization and regeneration cycles. A comparison study of benzene removal efficiency by ACF-TNW using combined process of oxidation and sorption with other sorbent/photo-catalysts was added in Table 1.

3.2.6. Photo-oxidation-sorption affinity mechanism

Scheme 1 shows the photo-oxidation and sorption affinity mechanism for improved benzene removal due to the porous carbon texture of ACFs and the generation of more electron-hole pairs in the ACF-TNW photocatalytic system under UV light irradiation and dark phase. The porous ACF substrate can improve the sorption affinity of benzene depending upon two main interactions: electrostatic and dispersive [20,22]. The dispersive attraction through π-π interactions between the π orbital of the ACFs surface on the car-

Please cite this article in press as: A. Sharma, B.-K. Lee, Growth of TiO_2 nano-wall on activated carbon fibers for enhancing the photocatalytic oxidation of benzene in aqueous phase, Catal. Today (2016), http://dx.doi.org/10.1016/j.cattod.2016.11.019

Table 1
Comparison of benzene removal efficiency by sorption/oxidation.

Catalyst/sorbent	Benzene (mg/L)	Removal efficiency (mg/g)	Removal efficiency (%)	Ref.
Granular activated carbon (GAC)	100	98.3	–	[29]
Carbon-nanoparticle polysulfone	100	67	–	[35]
ACF	10	66	–	[30]
TiO_2/zeolites	25	–	~100	[31]
Cu–TiO_2/PU	100	–	91	[9]
ACF-TiO_2	50	111.6	88.4	This study
ACF-TNW	50	144.8	98.7	This study

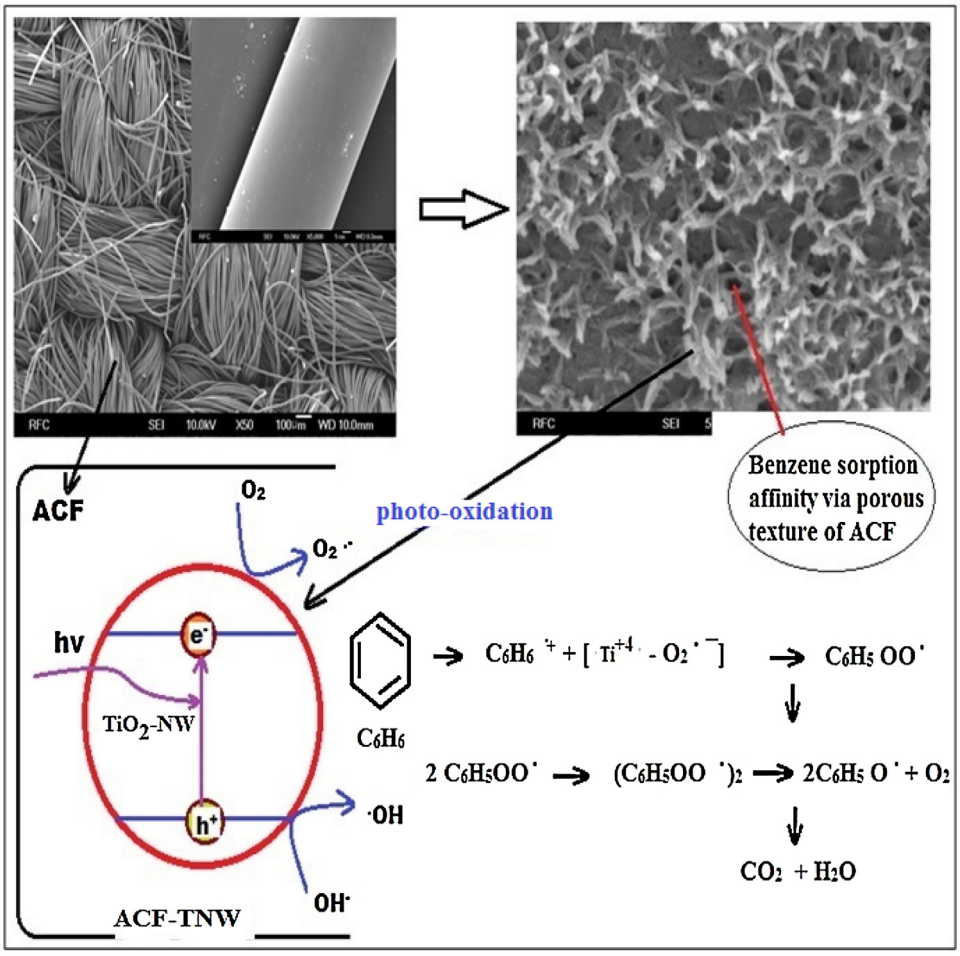

Scheme 1. Proposed schematic mechanism for the photo-oxidation of benzene by ACF-TNW.

bon basal planes and the electronic density in the benzene aromatic rings can improve the sorption affinity of benzene [35]. Furthermore, the electrostatic interaction between benzene molecules and the protonated structure of the ACF-TNW surface may also provide additional benzene sorption on ACFs. Yakout et Al. [40] suggested that benzene can also be adsorbed on the weakly acidic or nonacidic oxygen groups by the interaction of benzene ring π electrons with the positive charge of those groups. In the photo-oxidation of benzene by ACF-TNW under UV light irradiation, the ACF-TNW surface acts as a photocatalyst for benzene decomposition or mineralization. The positive holes of TiO_2 nano-wall break apart water molecules to form hydrogen and hydroxyl radicals, while the negative electrons react with oxygen molecules to form superoxide radicals. These hydroxyl radicals and superoxide radicals are efficient oxidants of photo-oxidation. The superoxide anion $O_2^{\bullet -}$, which can be formed via two different mechanisms on ACF-TNW, is a possible reactive species [39]. In the first case, the adsorption of oxygen on Ti^{+4} leads to the formation of a $(Ti^{+4} - O_2^{\bullet -})$ complex, as shown in Eq. (4);

$$Ti^{+4} + O_2 \rightarrow (Ti^{+4} - O_2^{\bullet -}) \quad (4)$$

The second possibility is the cleavage of $Ti^{+4} - O^{2-}$ peroxo-complexes in the presence of oxygen, as shown in Eq. (5):

$$Ti^{+4} + O_2^{2-}) + O_2 \rightarrow 2(Ti^{+4} - O_2^{\bullet -})^{+} \quad (5)$$

In these reactions, Ti^{+4} complexes can also be present in ACFs through high O—C and Ti—O—Ti bonding. Then the formed superoxide complex $(Ti^{+4} - O_2^{\bullet -})^{+}$ can react with a benzene radical cation from the benzene sorption to form a phenyl peroxy radical (see equation 6);

$$C_6H_6^{\bullet +} + (Ti^{+4} - O_2^{\bullet -})^{+} \rightarrow C_6H_5OO^{\bullet} \quad (6)$$

$$2C_6H_5OO^{\bullet} \rightarrow (C_6H_5OO)_2 \rightarrow 2C_6H_5O^{\bullet} + O_2 \quad (7)$$

Please cite this article in press as: A. Sharma, B.-K. Lee, Growth of TiO_2 nano-wall on activated carbon fibers for enhancing the photocatalytic oxidation of benzene in aqueous phase, Catal. Today (2016), http://dx.doi.org/10.1016/j.cattod.2016.11.019

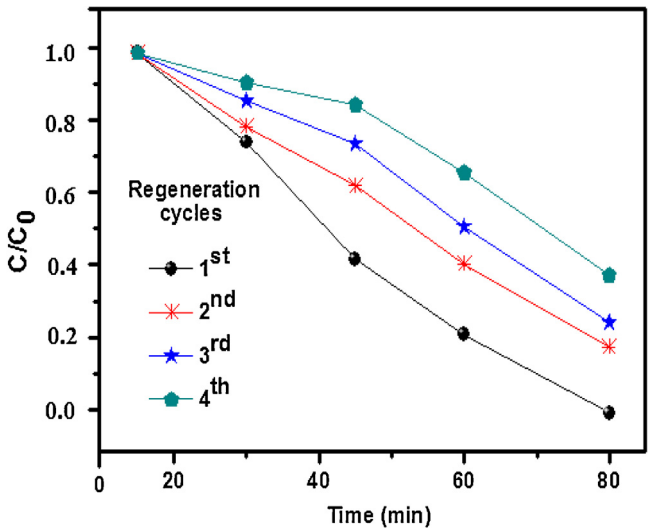

Fig. 10. Regeneration rate of ACF-TNW for the photo-oxidation of benzene. Concentration of benzene = 50 mg/L, amount of ACF-TNW = 2 cm × 2 cm, reaction volume = 100 mL, H_2O_2 = 0.1%, reaction time = 80 min, temperature = 30 °C.

Furthermore, phenyl peroxy radicals can dimerize via elimination of dioxygen to form phenoxy radicals, as shown in Eq. (7), which convert into phenol with the help of the TNW framework of ACFs [41]. Thus, phenol can be catalytically mineralized into CO_2 and water vapor [42]. Consequently, application of UV light to the reaction system results in the photo-oxidation of benzene with complete mineralization into CO_2 emission and TOC and COD reduction of 79.5% and 82.3%, respectively.

4. Conclusion

A stable TiO_2 nano-wall networks was uniformly grown on the ACFs surface. The sorption affinity of benzene on the ACF-TNW surface was enhanced due to the improved electrostatic and dispersive attraction. The more enhanced photocatalytic removal of benzene under UV light irradiation was attributed to the increased electron-hole pair separation efficiency through the ACFs surface in ACF-TNW. The maximum removal of benzene molecules (in 100 mL of 50 mg/L) was 111.6 and 144.8 mg/g for ACF-TiO_2 and ACF-TNW, respectively, at pH 5 under UV light irradiation within 80 min. The photo-oxidation of benzene was improved with H_2O_2 addition, which was attributed to the photo-Fenton catalytic reaction and photocatalytic reaction that occurred on the ACF-TNW surface. The photo-oxidation by ACF-TNW afforded a maximum benzene removal efficiency of 98.7%, with high CO_2 emission and TOC and COD reduction of 79.5% and 82.3%, respectively. ACF-TNW was easily collected from the solution even after multiple utilization/regeneration cycles and showed superior regeneration characteristics, including good phase stability.

Acknowledgements

This work was supported by a grant from the basic science research program through the National Research Foundation of Korea (NRF) funded by the Ministry of Education (2013R1A1A2065796) and (Grants No. C0398793) was supported by Business for Cooperative R&D between Industry, Academy, and Research Institute funded Korea Small and Medium Business Administration in 2016.

References

[1] T. Soltani, B.K. Lee, J. Hazard. Mater. 316 (2016) 122–133.
[2] Lyon, IARC Monographs on the Evaluation of the Carcinogenic Risk of Chemicals to Humans, 29 (1982) 93-148.
[3] W. Slooff, Integrated criteria document benzene, Public Health and Environmental Protection (Report No. 758476003) (1988).
[4] Office of Drinking Water. Benzene, US Environmental Protection Agency, (1987).
[5] Y. Xue, X. Gu, S. Lu, Z. Miao, M.L. Brusseau, M. Xu, X. Fu, X. Zhang, Z. Qiu, Q. Sui, Chem. Eng. J. 302 (2016) 187–193.
[6] W. Xiong, C. Mathies, K. Bradshaw, T. Carlson, K. Tang, Y. Wang, Water Res. 46 (2012) 4721–4731.
[7] Z. Zhang, Z. Jiang, W. Shangguan, Catal. Today 264 (2016) 270–278.
[8] R. Cheng, S. Shao, H. Wu, Y. Niu, J. Han, X. Zhao, Inorg. Chem. Commun. 46 (2014) 226–228.
[9] T.D. Pham, B.K. Lee, C.H. Lee, Appl. Catal. B: Environ. 182 (2016) 172–183.
[10] C.G. Silva, J.L. Faria, Appl. Catal. B: Environ. 101 (2010) 81–89.
[11] B. Dou, J. Li, Y. Wang, H. Wang, C. Ma, Z. Hao, J. Hazard. Mater. 196 (2011) 194–200.
[12] A. Sharma, B.K. Lee, J. Environ. Manage. 155 (2015) 114–122.
[13] O. Enachi, T. Lupan, A. Braniste, L. Sarua, D. Mishra, R. Gedamu, I. Tiginyanu, Phys. Status Solidi RRL 9 (3) (2015) 171–174.
[14] I. Dhada, P.K. Nagar, M. Sharma, Ind. Eng. Chem. Res. 54 (2015) 5381–5387.
[15] 2N-Y. K. Mishra, G., Modi, V., Cretu, V., Postica, O., Lupan, T., Reimer, I., Paulowicz, V., Hrkac, W., Benecke, L., Kienle, R. Adelung, ACS Appl. Mater. Interfaces, 7, (2015), 14303–14316.
[16] T. Reimer, I. Paulowicz, R. Roder, S. Kaps, O. Lupan, S. Chemnitz, W. Benecke, C. Ronning, R. Adelung, Y.K. Mishra, ACS Appl. Mater. Interfaces 6 (2014) 7806–7815.
[17] F. Moulis, J. Krysa, Catal. Today 209 (2013) 153–158.
[18] B. Bhaduri, N. Verma, J. Colloid Interface Sci. 436 (2014) 218–226.
[19] M. Mecklenburg, A. Schuchardt, Y.K. Mishra, S. Kaps, R. Adelung, A. Lotnyk, L. Kienle, K. Schulte, Adv. Mater. 24 (2012) 3486–3490.
[20] J.W. Shi, H.J. Cui, J.W. Chen, M.L. Fu, B. Xu, H.Y. Luo, Z.L. Ye, J. Colloid Interface Sci. 388 (2012) 201–208.
[21] Y. Ao, J. Xu, Y. Gao, P. Wang, C. Wang, J. Hou, J. Qian, Catal. Commun. 53 (2014) 21–24.
[22] G.B. Baur, I. Yuranov, L. Kiwi-Minsker, Catal. Today 249 (2015) 252–258.
[23] A. Wei, B. Liu, H. Zhao, Y. Chen, W. Wang, Y. Ma, H. Yang, S. Liu, Chem. Eng. J. 239 (2014) 141–148.
[24] J.W. Shi, Chem. Eng. J. 151 (2009) 241–246.
[25] J. Shi, J. Zheng, P. Wua, X. Ji, Catal. Commun. 9 (2008) 1846–1850.
[26] B. Weng, F. Xu, F. Yu, Mater. Lett. 145 (2015) 70–73.
[27] S. Ayissi, P.A. Charpentier, K. Palota, N. Farhangi, F. Schwarz, W.A. Hofer, J. Phys. Chem. C 119 (2015) 15085–15093.
[28] A. Sharma, B.K. Lee, J. Environ. Manage. 165 (2016) 1–10.
[29] N. Wibowo, L. Setyadhi, D. Wibowo, J. Setiawan, S. Ismadji, J. Hazard. Mater. 146 (2007) 237–242.
[30] Z. Yue, C. Mangun, J. Economy, Environ. Sci. Technol. 35 (2001) 2844–2848.
[31] H. Huang, G. Liu, Y. Zhan, Y. Xu, H. Lu, H. Huang, Q. Feng, M. Wu, Catal. Today (2016), in press http://dx.doi.org/10.1016/j.cattod.2016.07.005.
[32] S.Y. Ye, M.B. Li, X.L. Song, S.C. Luo, Y.C. Fang, Chem. Eng. J. 167 (2011) 28–34.
[33] R. Yuan, R. Guan, P. Liu, J. Zheng, Colloid Surf. A 293 (2007) 80–86.
[34] P. Wu, L. Xia, M. Dai, L. Lin, S. Song, Colloid Surf. A 502 (2016) 66–73.
[35] R. Mukherjee, S. De, Sep. Purif. Technol. 157 (2016) 229–240.
[36] M. Laabd, A.E. Jaouhari, M.A. Haki, H. Eljazouli, M. Bazzaoui, H. Kabli, A. Albourine, J. Environ. Chem. Eng. 4 (2016) 1869–1879.
[37] X. Fu, X. Gu, S. Lu, Z. Miao, M. Xu, X. Zhang, Z. Qiu, Q. Sui, Chem. Eng. J. 267 (2015) 25–33.
[38] J.A. Khan, X. He, N.S. Shah, H.M. Khan, E. Hapeshi, D. Fatta-Kassinos, D.D. Dionysiou, Chem. Eng. J. 252 (2014) 393–403.
[39] C. Ren, W. Qiu, H. Zhang, Z. He, Y. Chen, J. Mol. Catal. A Chem. 398 (2015) 215–222.
[40] S.M. Yakout, Chem. Cent. J. 8 (52) (2014) 1–7.
[41] F. He, J. Li, T. Li, G. Li, Chem. Eng. J. 237 (2014) 312–321.
[42] J. Wang, X. Wang, X. Liu, T. Zhu, Y. Guo, H. Qi, Catal. Today 241 (2015) 92–99.

Please cite this article in press as: A. Sharma, B.-K. Lee, Growth of TiO_2 nano-wall on activated carbon fibers for enhancing the photocatalytic oxidation of benzene in aqueous phase, Catal. Today (2016), http://dx.doi.org/10.1016/j.cattod.2016.11.019